Article

Current Biology

Directional tuning in the hippocampal formation of birds

Highlights

- Nearly 12% of the cells in the hippocampus of quails are modulated by the head direction
- The preferred directions are stable over time, speed, and location
- The preferred directions cover uniformly all directions
- Place cells and border cells are generally not encountered

Authors

Elhanan Ben-Yishay, Ksenia Krivoruchko, Shaked Ron, Nachum Ulanovsky, Dori Derdikman, Yoram Gutfreund

Correspondence

yoramg@technion.ac.il

In brief

Ben-Yishay et al. report single-neuron recordings in the hippocampal formation of freely roaming quails. They show, for the first time in an avian species, stable head-direction tuning—providing a basis for a comparative study of the hippocampus and its role in the control of spatial behaviors across vertebrates.

Ben-Yishay et al., 2021, Current Biology *31*, 1–11
June 21, 2021
https://doi.org/10.1016/j.cub.2021.04.029

CellPress

Current Biology

CellPress

Article

Directional tuning in the hippocampal formation of birds

Elhanan Ben-Yishay,[1,3] Ksenia Krivoruchko,[1,3] Shaked Ron,[1] Nachum Ulanovsky,[2] Dori Derdikman,[1] and Yoram Gutfreund[1,4,*]

[1]Department of Neurobiology, Rappaport Research Institute and Faculty of Medicine, Technion - Israel Institute of Technology, 1 Efron Street, Haifa 3525422, Israel

[2]Department of Neurobiology, Weizmann Institute of Science, Rehovot 76100, Israel

[3]These authors contributed equally

[4]Lead contact

*Correspondence: yoramg@technion.ac.il

https://doi.org/10.1016/j.cub.2021.04.029

SUMMARY

Birds strongly rely on spatial memory and navigation. Therefore, it is of utmost interest to reveal how space is represented in the avian brain. Here we used tetrodes to record neurons from the hippocampal formation of Japanese quails—a ground-dwelling species—while the quails roamed in an open-field arena. Whereas spatially modulated cells (place cells, grid cells, border cells) were generally not encountered, the firing rate of about 12% of the neurons was unimodally and significantly modulated by the head azimuth—i.e., these were head-direction cells (HD cells). Typically, HD cells were maximally active at one preferred direction and minimally at the opposite null direction, with preferred directions spanning all 360° across the population. The preferred direction was independent of the animal's position and speed and was stable during the recording session. The HD tuning was broader compared to that of HD cells in rodents, and most cells had non-zero baseline firing in all directions. However, similar to findings in rodents, the HD tuning usually rotated with the rotation of a salient visual cue in the arena. Thus, these findings support the existence of an allocentric HD representation in the quail hippocampal formation and provide the first demonstration of HD cells in birds.

INTRODUCTION

Since the seminal discovery of place cells in the rat hippocampus,[1,2] research on mammalian hippocampal formation (HPF) has been one of the most active fields in neuroscience. Half a century of extensive research has resulted in a detailed characterization of hippocampal space processing in rodents, and advanced the development of new techniques and paradigms for neural recording in behaving animals, as well as new theories and ideas on the functional role of the hippocampus.[3] In addition to place cells, a whole range of other spatial cell types have been discovered in mammals, including head-direction (HD) cells,[4] spatial-view cells,[5] grid cells,[6] border cells,[7,8] speed cells,[9] and, recently, goal-direction cells.[10] The study of spatial processing in the hippocampus was not limited to rats but expanded to other mammals, including mice, bats, monkeys, and humans.[11–16] The emerging notion is that the hippocampus and its related structures support spatial cognition and memory.[17–19]

One important and relatively understudied question is whether the role of the HPF in spatial cognition is unique to mammals, or whether we can find its origins in other vertebrates. In this aspect, birds provide an interesting case study. Spatial navigation and foraging behaviors are common in avian species, and in some cases outperform those of mammals. Migratory and homing behaviors are stunning examples of bird navigational capabilities.[20–24] In addition, the extraordinary food-caching and retrieval behaviors found in some songbird species demonstrate the impressive spatial-memory capacities of birds.[25–28] What might be the neural mechanisms that support such elaborate spatial cognition in birds? And how similar are they to the hippocampal space-processing system in mammals? Answers to these questions will constitute a breakthrough in our understanding of the evolutionary origin of space processing and, through comparative studies, may contribute to understanding the underlying mechanisms and to establishing general principles of navigation and spatial memory across vertebrates.

The avian HPF, a structure in the dorsal medial cortex of the avian brain (Figure 1), is considered to be the homolog of the mammalian hippocampus, based on developmental, topographical, genetic, and functional lines of evidence.[29–33] Yet striking differences exist between the avian HPF and the mammalian HPF with regard to internal organization and external connections.[29,34] Moreover, theta oscillations, a distinct hippocampal rhythm in rodents, seem to be absent from the avian hippocampus[35] (but see Siegel et al.,[36] who reported short theta bouts in pigeons). Despite the apparent differences, growing evidence suggests that, like its mammalian counterpart, the avian HPF plays a key role in spatial tasks and episodic memory.[21,24,27,29] For example, experiments in HPF-lesioned pigeons consistently showed deficits in homing behaviors.[37] Similarly, lesion studies in zebra finches demonstrated that the HPF in these songbirds is involved in both learning and retention of

Please cite this article in press as: Ben-Yishay et al., Directional tuning in the hippocampal formation of birds, Current Biology (2021), https://doi.org/10.1016/j.cub.2021.04.029

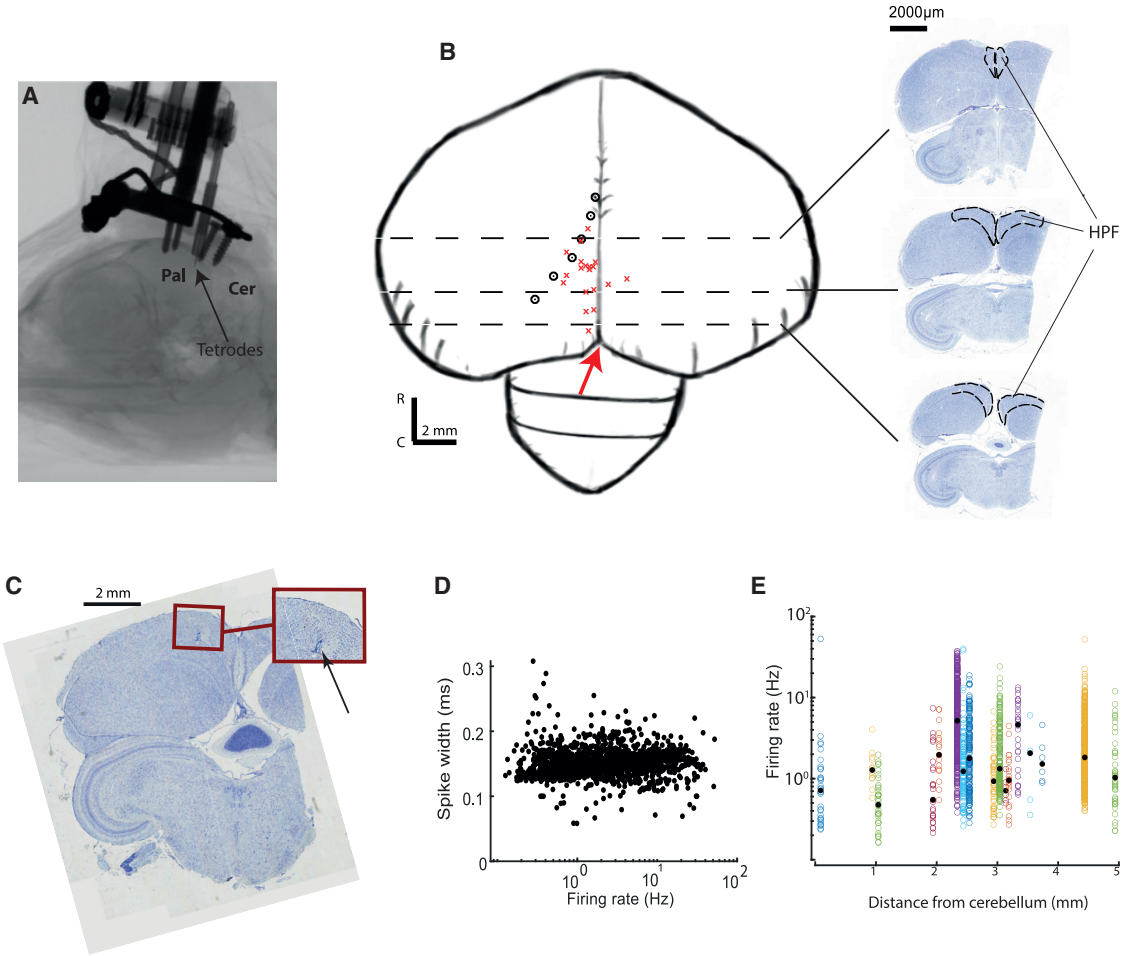

Figure 1. Recording locations and firing properties

(A) Micro-CT scan showing an implanted microdrive on the quail's skull. The arrow points to the tip of the tetrodes. Pal, pallium; Cer, cerebellum.

(B) A sketch of the quail's brain. Red X's mark the approximate recording locations from 19 quails (Table S1). Black dots represent the putative lateral border of the hippocampal formation (HPF), which follows the lateral end of the lateral ventricle. Distances of black circles from the midline are approximated based on figures from the quail's brain stereotaxic atlas.[45] Dashed lines indicate the approximate coronal section levels shown on the right. The dashed lines in the insets mark the HPF. The red arrow denotes the cerebellum tip.

(C) A Nissl-stained coronal section showing an electrolytic lesion. Inset: magnified view of the lesioned region. The arrow points to the lesion mark.

(D) Spike width (full width at half maximum) for all the recorded single units as a function of their firing rate. The x axis is logarithmic.

(E) Firing rates of single units versus the recording location along the rostro-caudal axis (rostral distance from the cerebellum tip). Colors designate different quails. Black circles designate the median firing rates. The y axis is logarithmic.

See also Table S1.

spatial tasks.[38] Investigations of immediate-early gene expression patterns showed enhanced activation of the HPF during retrieval of cached food items[39]—a highly demanding spatial behavior—as well as during maze tasks.[40] Another striking indication for the involvement of avian HPF in spatial memory is found in the correlation between HPF volume and the importance of food caching for the natural behavior of the species.[41] Finally, neurons with place fields were reported in the pigeon HPF, although these fields were mostly associated with rewarded locations.[42–44] These raise the hypothesis that the role of the mammalian hippocampus in spatial cognition, and the underlying neural spatial representation (place cells, grid cells, HD cells, etc.), has its roots in earlier vertebrate evolution. However, a clear allocentric representation of space, akin to that found in mammalian species, has not been reported yet in either the avian hippocampus or in any other non-mammalian vertebrate.

In this study, we report results of single-unit recordings in the HPF of Japanese quails (*Coturnix japonica*). The Japanese quail is a ground-dwelling foraging bird, which has been extensively used as an animal model in developmental biology.[46] However, to our knowledge, single-unit recordings in behaving quails have not been done before. The natural ground-foraging behavior of quails in relatively small areas[47] is reminiscent of the rodents' small-scale foraging behavior. We therefore asked whether the resemblance of foraging behavior between quails and rodents implies resemblance in spatial representation. To this end, we used tetrode microdrives to perform electrophysiological recordings in freely behaving quails as they explored a square

Please cite this article in press as: Ben-Yishay et al., Directional tuning in the hippocampal formation of birds, Current Biology (2021), https://doi.org/10.1016/j.cub.2021.04.029

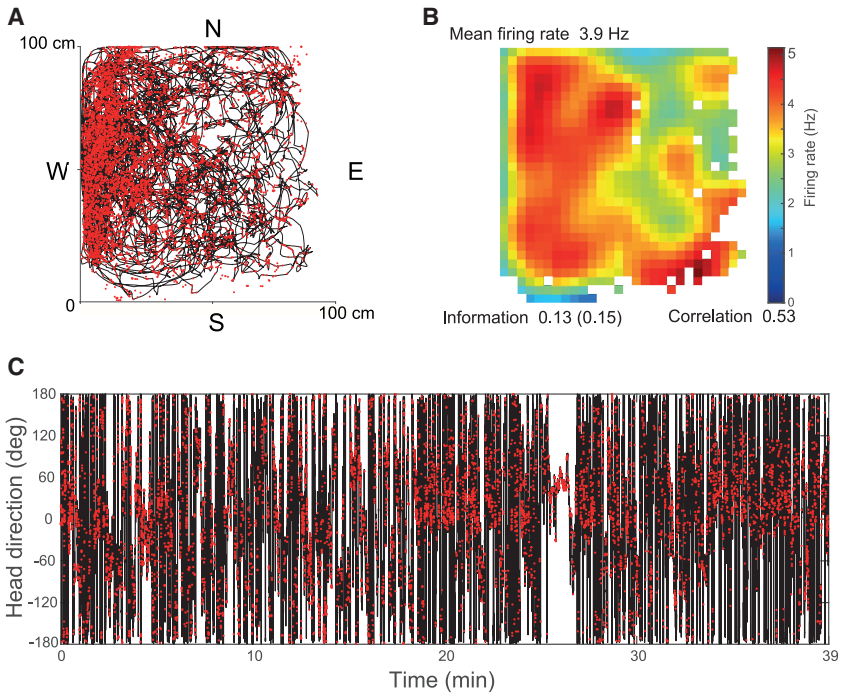

Figure 2. Data from an example neuron

(A) The quail's position in the arena during a 35-min recording session is marked by a black line. Red dots are the locations of spikes fired by the neuron. N, north side of the arena; S, south; E, east; W, west.

(B) Firing-rate map of the neuron. Indicated are the mean firing rate (top left), spatial information in bits/spike (bottom left), and map correlation between the first and second halves of the session (bottom right). White pixels are pixels that were not visited for at least 200 ms during the session. See Figure S2 for more examples of firing-rate maps.

(C) Head direction of the quail as a function of time (black line), with spike times superimposed (red dots).

(D) Polar plot showing the firing rate as a function of head direction (blue). The red bar indicates the length and direction of the Rayleigh vector. The black curve shows the relative time spent behaviorally in each head-direction bin.

(E) Rayleigh vector shuffling histogram. The red dashed line represents the Rayleigh vector length for the 99% percentile shuffle; the green line shows the observed Rayleigh vector length for this example neuron.

See also Figures S1 and S2.

arena, while we tracked their position and head direction. Analysis of more than 2,000 single units in the HPF did not reveal clear spatially modulated cells (e.g., place cells). However, we found that about 12% of the recorded cells showed a statistically significant (yet broad) HD response, which maintained directional stability over time, space, and speed, and rotated with a salient visual cue. We thus provide the first evidence for an HD system in an avian species, shedding new light on the evolutionary and functional homology of the hippocampal system across taxa.

RESULTS

No evidence for rodent-like place cells in the HPF of quails

We recorded and isolated 2,316 single units from 23 quails. In several of the quails, the signal-to-noise levels of the units were substantially reduced in the days following the surgery—and hence the large variation in the number of cells collected from each quail—from 4 cells in quail 30 to 514 cells in quail 24 (Table S1). Tetrodes were implanted in the left hemisphere in 21 out of the 23 quails and were stereotactically targeted to a zone within 5 mm rostral from the cerebellar rostral tip, and within 2 mm lateral to the midline (Figures 1A and 1B). We targeted mostly the left HPF because of previous studies that reported functional lateralization in the HPF of pigeons, with the left side more involved in the representation of spatial parameters.[44,48] Nineteen locations of tetrode positioning were reconstructed post-mortem by measuring the rostral and lateral distances of the tetrode penetration sites from the rostral tip of the cerebellum (Figure 1B). In 4 quails, the tetrode track was additionally reconstructed with an electrolytic lesion (Figure 1C). In two of the birds, tetrode tracks were reconstructed from computed microtomography (micro-CT) scans (Figure 1A). Across the recorded population, firing rates and spike widths varied; but we could not detect systematic clustering of cell spike types (Figure 1D) nor systematic variation of firing rates along the rostro-caudal axis (Figure 1E).

During the experiments, the quails sometimes explored the arena relatively evenly and sometimes in a restricted manner (Figures 2A and S1). In many cases, such as the example cell shown in Figure 2, the firing rate as a function of the quail's position (rate map) displayed broad spatial firing across the arena (Figure 2B). In this example cell, spatial information was not

Please cite this article in press as: Ben-Yishay et al., Directional tuning in the hippocampal formation of birds, Current Biology (2021), https://doi.org/10.1016/j.cub.2021.04.029

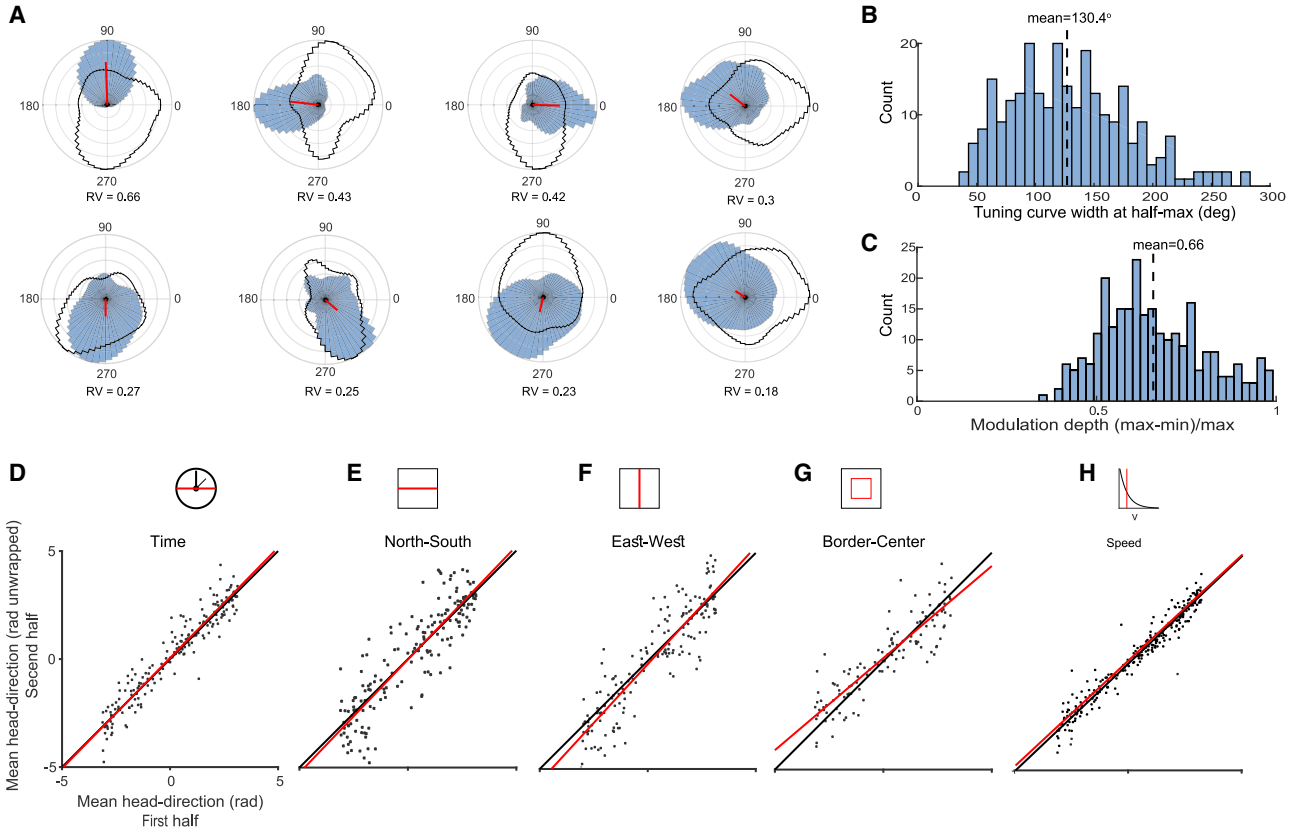

Figure 3. HD cell characteristics and stability

(A) Examples of eight cells significantly modulated by head direction, organized in descending order by their Rayleigh vector (RV; its value is indicated below each neuron). Blue histograms represent the polar firing-rate curve. The black line depicts the time spent in each direction (behavioral curve). Curves are normalized to their maximum.

(B) Distribution of the tuning-curve widths (width at half maximum) of the HD firing-rate curves. The dashed line represents the population mean.

(C) Distribution of the modulation depths (maximal firing rate of the tuning curve minus the minimal firing rate, normalized by the maximal firing rate). The dashed line represents the mean. See Figure S3 for the distribution of the Rayleigh scores, skewness, modulation depth, width, and mean firing rate in quails and rats.

(D–H) Population scatterplots for HD cells, comparing the preferred head directions in the first half versus the second half of the session (D), north versus south parts of the arena (E), east versus west parts of the arena (F), near border versus center of the arena (G), and fast speeds versus slow speeds (H). Black lines are the identity lines (equal preferred directions) and red lines show the linear regressions.

See also Figures S1 and S3.

statistically significant. Only 19 cells out of 938 cells that were recorded in behavioral sessions where the quail covered more than 50% of the arena have passed the criterion for place cells (spatial information larger than the 99th percentile of the shuffles; $p < 0.01$). This constitutes 2% of the cells, which is barely above the chance level of 1%. Moreover, these neurons mostly did not display a clear single field of activity in their rate maps (Figure S2). Therefore, we did not pursue further analysis of place modulations in this study.

HD cells in the HPF of quails

We next moved to analyzing the relationship between the firing rate and the head direction. In the example cell, firing rate was clearly modulated by the head direction (Figure 2C), rising from 2 Hz at 180° azimuth to more than 6 Hz at 10° azimuth (Figure 2D). The Rayleigh vector length (STAR Methods; termed hereafter "Rayleigh vector") of the cell was 0.217; when compared to 1,000 shuffled (randomly time-shifted) spike trains, the observed Rayleigh vector was well above the 99th percentile of the shuffled distribution (Figure 2E)—and thus we categorized this example cell as having a significant HD response ($p < 0.01$). The preferred direction of the response (computed as the direction of the Rayleigh vector) pointed roughly north-east (red bar in Figure 2D).

Out of the recorded population, 260 cells (~12%) passed the shuffling statistical test as HD cells, with a chance level of 1% (Table S1). To confirm that the number of HD cells is not biased by the parameters used to define a single unit (isolation distance and L-ratio criteria; STAR Methods), we analyzed the percentage of HD cells at 8 different combinations of criteria (Table S2). The value of roughly 12% HD cells was maintained regardless of the combination of criteria used.

Stability and distribution of preferred directions

In general, the HD modulation tended to be relatively broad (Figure 3A). The mean tuning width (width at half height, measured halfway between the maximum and minimum of the tuning) for the population of significant HD cells was 130.4° ± 54° (Figure 3B; mean ± SD; standard deviation). Moreover, the modulation

Please cite this article in press as: Ben-Yishay et al., Directional tuning in the hippocampal formation of birds, Current Biology (2021), https://doi.org/10.1016/j.cub.2021.04.029

depth (normalized difference between the highest and lowest firing rates) varied between 0.4 and 1, with a mean of 0.66 (Figure 3C). To compare these mean values with the corresponding values of HD cells in rodents, we performed the same analyses on datasets of previously recorded neurons from the medial entorhinal cortex (MEC), parasubiculum (PaS), and dorsal presubiculum (dPrS) of rats, areas that are well known for their robust representation of head direction (data from Gofman et al.[49] and Boccara et al.[50]). Out of the 2,404 cells from rats that we analyzed, 1,046 were significant HD cells, comprising 44% (compared to 12% in the quails' HPF). The distribution of widths at half height, the SDs of the rate curves, and the Rayleigh vectors of HD cells all pointed to substantially narrower tuning of rat HD cells as compared to quail HD cells (Figure S3). Moreover, the mean modulation depth of the HD cells in rats was substantially larger compared to the HD cells in quails (0.85 compared with 0.66 in quails; Figure S3).

Despite their relatively broad shape, the HD tuning curves in the quails had high directional stability, as follows. (1) The preferred directions in the first and second halves of the session were significantly correlated (Figure 3D; Pearson correlation: $r = 0.95$, $p < 0.0001$, $n = 186$; the numbers of neurons in this and the following comparisons are lower than $n = 260$ because we required sufficient coverage in both halves; STAR Methods). (2) The preferred directions computed from the north versus south halves of the arena were significantly correlated (Figure 3E; Pearson correlation: $r = 0.88$, $p < 0.0001$, $n = 175$), and likewise for preferred directions from the west versus east halves (Figure 3F; Pearson correlation: $r = 0.90$, $p < 0.0001$, $n = 169$). (3) Because some of the quails mostly explored the borders of the arena (see examples in Figure S1), we also analyzed the preferred head directions when the quails were near the border versus when they were in the center of the arena; these were also found to be highly significantly correlated (Figure 3G; Pearson correlation: $r = 0.88$, $p < 0.0001$, $n = 122$). (4) Finally, the preferred directions during fast movement of the quail (>5 cm/s) were significantly correlated with the preferred directions during slow movements (<5 cm/s) (Figure 3H; Pearson correlation: $r = 0.97$, $p < 0.0001$, $n = 260$). In all these tests, the regression line was very close to the 45° line (Figures 3D–3H, compare red and black lines). Our results indicate a stable HD representation over time and space, as well as over the speed of the quails. The significant correlation between the preferred directions in different parts of the arena argues against the possibility that the HD tuning is an outcome of spatial-view cells.[5]

In rodents, HD cells commonly rotate their preferred direction following rotation of salient cues in the arena.[4,51] We therefore positioned, in some of the experiments, two LED light sources in opposite sides of the arena, lit only one of them, and then switched the side of the illuminating source at mid-session (STAR Methods). 45 significant HD cells (41 from quail 66 and 4 from quail 70; Table S1) in 10 recording sessions were analyzed in this experiment. Following the switch, many of the neurons demonstrated clear 180° rotation of their tuning curve (Figure 4A). At the population level, the distribution of the preferred-direction differences between light on one side and light on the 180°-opposite side was centered near 180° (Figures 4B and 4C; mean angle ± circular SD = 170° ± 56°), and significantly deviated from the distribution of the mean directional shift between the two halves of the session without cue changes (Figures 4B and 4C; Watson-Williams mean angle test, $p < 0.0001$). As can be seen in the distribution of the preferred-direction differences (Figure 4C), the majority of the neurons rotated their preferred direction by close to 180°. However, a small subset of neurons did not shift or only mildly shifted their preferred direction (example in Figure 4D) or shifted in between 0° and 180° (example in Figure 4E).

The preferred directions of the population covered almost uniformly the entire range of 360°. This uniformity was seen when pooling data from all quails (Figure 5A), as well as in most of the individual quails (Figure S4). Significant HD cells, spanning all possible directions, have been recorded at all the recording depths in the HPF and at all anatomical locations within the HPF (Figures 5B and 5C). HD cells were found at nearly all depths from the brain surface, and all distances rostral to the cerebellum tip (Figures 5D and 5E). Thus, our results do not indicate a clear tendency for anatomical clustering of HD cells or anatomical clustering of preferred directions. We conclude that significant and stable HD cells are found throughout the HPF of quails.

DISCUSSION

To our knowledge, this is the first time that a stable and abundant population of head-direction-tuned cells is reported in the HPF of an avian species. Neurons that represent head direction in allocentric coordinates during real-world movements have been reported in mammals,[4,52–54] and very recently in fish[55]—as well as in head-fixed insects in virtual reality.[56,57] These cells are thought to underlie the directional sense of animals, which is vitally important for goal-directed navigation and other spatially coordinated behaviors.[58] Because many species of birds display remarkable cognitive capabilities that are related to spatial behaviors and spatial memory,[20–24,26] an elaborated HD system is expected in avian brains. However, up until now, such a system has not been discovered. A characteristic of mammalian systems representing head direction is that they exhibit a uniform and stable representation of directions.[58,59] Moreover, direction sensitivity is maintained independent of the speed of the animal.[4] Here we report a population of neurons that are modulated by the head direction of the quail: these neurons uniformly represent all directions, and their preferred direction is stable across time, space, and movement speeds. We therefore posit that these cells are part of an HD system in quails, perhaps homologous to that of mammals.

In rodents, HD cells were shown to maintain tuning and preferred directions even after switching from light to complete darkness,[60] ruling out the possibility that the HD tuning reflects purely visual responses to a landmark in the environment.[61] In quails, this manipulation is not possible because, in darkness, quails tend to stay motionless in one position. Yet several observations in our data suggest that simple visual responses cannot explain the directional tuning, as follows. (1) The tuning direction was not influenced by the quail's location in the arena (Figures 3E–3G). (2) HD tuning was found both when the light source was in the ceiling above the arena (the standard experiments) as well as when the light came from the side (light-rotation experiments). (3) HD cells tuned to all possible directions shifted their preferred direction when the light direction was shifted (not only

Please cite this article in press as: Ben-Yishay et al., Directional tuning in the hippocampal formation of birds, Current Biology (2021), https://doi.org/10.1016/j.cub.2021.04.029

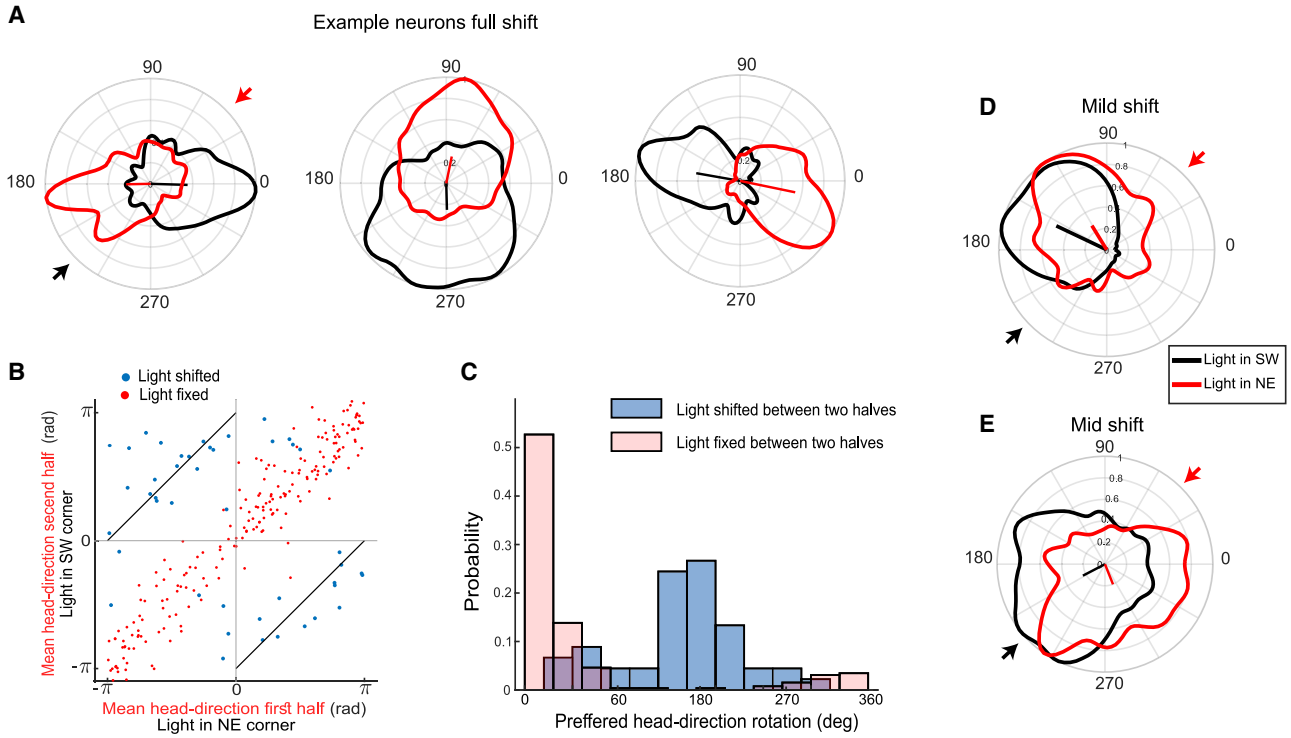

Figure 4. Response of HD cells to cue rotation

(A) Examples of HD tuning curves of three cells before and after 180° cue rotation (light-source shift). Red curves were measured when the light source was in the north-east corner of the arena and black curves when the light source was in the south-west corner (the arrows in the left panel designate the directions of the light sources in the arena). Straight lines originating from the center designate the directions and lengths of the corresponding Rayleigh vectors.

(B) Preferred head directions in the second half of the session are plotted versus the preferred head directions in the first half of the session. The blue dots show the results when the light source was shifted at mid-session by 180°. For comparison, superimposed in red are the dots from Figure 3D to show the result without a cue shift. The black diagonal lines indicate the predicted 180° shift of the preferred direction.

(C) Distribution of the differences between preferred head directions measured in the two halves of the session, when the light was shifted by 180° (blue), compared to no shift (pink).

(D) Example of an HD cell whose tuning did not shift direction with the light-source shift. Plotted as in (A).

(E) Example from a different neuron showing an HD tuning curve that shifted about halfway from the predicted shift. Plotted as in (A).

those cells that pointed to the visual cue)—arguing against a purely visual response. However, further studies of manipulating the environment and/or the animal's movement are required in order to elucidate how the HD signal discovered here is affected by different sensory modalities.

Networks of HD cells in mammals integrate angular velocity information coming from the vestibular system with environmental cues from the visual system.[62] This integration is believed to take place in the dPrS,[63] anterodorsal thalamus, and lateral mammillary nucleus.[64] The HD information is conveyed from the dPrS to the entorhinal cortex, where it interacts with other spatial information coming from the hippocampus.[65,66] In addition, HD cells have been found in the PaS, MEC, and retrosplenial cortex,[67,68] where responses are shaped more by visual landmarks than by self-motion cues. The latter are believed to facilitate anchoring of HD signals to visual landmarks.[68] The sub-division homology between the avian HPF and the mammalian HPF is not well established.[29] Atoji and Wild[31,69] provided a histochemical division of the pigeon HPF to the dorsal lateral (DL), dorsal medial (DM), and a medial V-shaped complex. The homology of this sub-division with the mammalian HPF is debated, with the controversy focused mostly around the homologies of the V-shaped complex and the DM parts with the mammalian dentate gyrus and Ammon's horn.[70–74] However, there seems to be an agreement regarding the avian DL being related to the mammalian subiculum complex and entorhinal cortex.[29,31,34,75,76] Many of the HD cells that we recorded were in the more accessible DL and DM parts of the HPF (Figures 1B and 5B)—thus, our findings possibly represent an avian HD system homologous to the parahippocampal HD system of mammals. Notably, the DL and DM portions of the HPF receive connections from the visual wulst[77] as well as connections from the dorsal thalamus,[78] which may provide the anatomical substrates for integration of visual and self-motion cues. Further studies are required to establish whether the HD cells found here rely on the integration of self-motion cues from thalamic and brainstem nuclei, as was found in the mammalian dPrS,[79] or primarily rely on visual landmarks, as was found in retrosplenial cortex and some neurons in the PaS and MEC.[68]

Obvious differences exist between our findings and analogous reports in rodents, as follows. (1) Many of the HD cells in the entorhinal cortex and dPrS of mammals fire close to zero spikes (<0.5 Hz) in the null directions,[80,81] whereas in our population of HD cells the neurons had a non-zero baseline firing at all

Please cite this article in press as: Ben-Yishay et al., Directional tuning in the hippocampal formation of birds, Current Biology (2021), https://doi.org/10.1016/j.cub.2021.04.029

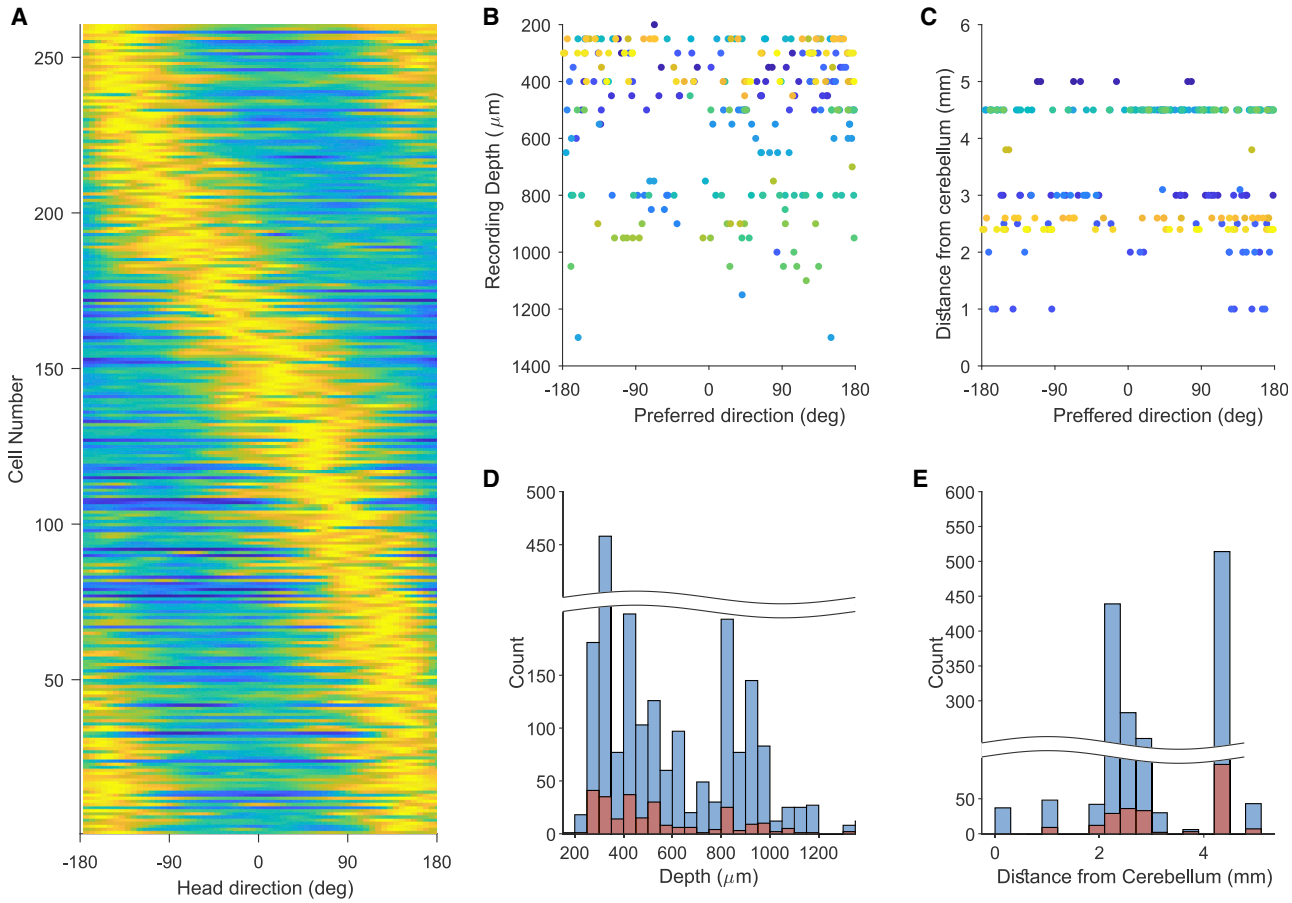

Figure 5. Distribution of preferred directions across the population of HD cells

(A) Normalized HD tuning curves for all significant HD cells, ordered according to the preferred direction. See Figure S4 for the normalized HD tuning curves in individual quails.

(B) Preferred directions of HD cells as a function of estimated recording depth. Colors designate different quails.

(C) Preferred directions as a function of recording distance from the cerebellum along the rostro-caudal axis. Colors indicate different quails.

(D) Histograms of the total number of single units (blue) and the number of HD cells (orange) as a function of recording depth.

(E) Same as (D) but plotted as a function of recording distance from the cerebellum.

See also Figure S4 and Table S1.

head directions, with significantly higher rates in the preferred direction as compared to the null directions. (2) Many neurons in the PrS and MEC of rodents are narrowly tuned (<45° width at half peak).[80] Such narrowly tuned neurons were a small fraction of our population of HD cells, whereas most of the quail's HD cells were more broadly tuned. (3) The proportion of HD cells in the avian HPF was lower than in the mammalian dPrS and layers III to VI of the MEC, where more than 40% of the neurons are significant HD cells,[50,81] compared to about 12% of the recorded cells in the quail. These differences between findings in quails and rodents are not a reflection of different metrics used in different papers, because we repeated the analysis on raw data of populations of neurons recorded from rats in the PaS, dPrS, and MEC[49,50]—using the exact same analysis pipeline—and have confirmed the substantial differences in modulation depth, tuning broadness, and abundance of HD cells (Figure S3). The relatively low abundance of HD cells in our findings may reflect the non-focal sampling of neurons in our study: perhaps a higher fraction of HD cells would be found in specific sub-regions of the HPF. However, our results showed no clear evidence for anatomical clustering of HD cells in the quail's HPF (Figures 5D and 5E).

Functional hemispheric lateralization is common in birds with laterally placed eyes.[82] Recordings in the pigeon HPF demonstrated a significant difference in the activity of neurons between the two hemispheres: neurons in the left HPF tended to code spatial parameters more reliably, whereas neurons in the right HPF tended to code goal locations.[44] Lateralization of HPF spatial coding is also supported by a lesion study in pigeons showing that an intact left but not right HPF is required for using local landmarks to guide food search.[48] Following these studies, we performed most of our recordings in the left hemisphere. However, we did record in two quails from the right hemisphere (quails 15 and 70; Table S1) and found 15 HD cells out of 130 cells (11%). Thus, we have no indication for lateralized organization of HD cells in the quail. However, further sampling is required for a thorough comparison between hemispheres.

Please cite this article in press as: Ben-Yishay et al., Directional tuning in the hippocampal formation of birds, Current Biology (2021), https://doi.org/10.1016/j.cub.2021.04.029

Another striking difference between neural responses in rodents and the results reported here is the apparent lack of clear place cells, grid cells, and border cells. A small number of neurons showed spatial modulation of their firing rates, but these were mostly broadly tuned (Figure S2). These results are consistent with results reported by Bingman and colleagues,[42–44] who studied the HPF of pigeons in radial mazes and open arenas. These previous studies found cells that were significantly spatially modulated, but in many cases the responses were consistent with multiple broad fields and were related mostly to rewarded locations. In particular, spatially modulated signals were scarce in pigeons foraging in open arenas without stable goals (comparable to our experiment).[43] A preliminary electrophysiological survey of zebra finch HPF also identified scarce place cells with relatively broad spatial tuning.[83] On the other hand, behavioral experiments in quails,[84] pigeons,[85] and zebra finches[86] strongly support well-developed spatial cognitive abilities in these bird species—such as novel shortcuts, model-based spatial learning, navigation, and spatial memory. Thus, the relative lack of place cells in our data and in data from other avian species remains a puzzle that is not likely to be accounted for by differences in behavior between birds and rodents, as here we recorded from birds freely roaming a square arena, similar in size and in recording conditions to many experiments in rats and mice that showed clear place cells and grid cells.[50,87] Another possible explanation for the differences in spatial representation may stem from the fact that rodents strongly rely on somatosensation and olfaction,[88,89] whereas quails and many other species of birds are primarily visual.[90] Yet the findings of place cells in flying bats both when using vision and when using echolocation[91] strongly suggest that, across species, the existence of place cells is not directly correlated with the dominant sensory modality of the species. Another possibility is that the neural substrate of spatial perception of birds is not localized in the HPF or, alternatively, it is localized in a specific sub-region of the HPF that has not been explored yet. However, lesion studies in quails, pigeons, and zebra finches,[38,92,93] as well as gene expression analyses,[94,95] provide strong evidence that the HPF is critically important for spatial cognition. Moreover, a very recent preliminary study in food-caching birds that are specialized in spatial memory (tufted titmouse) revealed place cells in the rostral HPF,[83] in the same areas that have been explored in other birds, including here in quails—but without observing place cells. This strongly suggests the notion that the HPF in birds generally supports spatial cognition—but that the detailed coding scheme is species specific and evolved differently according to the ecological needs of the species. Rather than having a large population of highly specific and sparsely encoding spatial cells—as seen in mammals—quails might possess a population-coding scheme that is carried out by a population of neurons with broad tuning and non-uniform fields. This possibility is consistent with our findings of HD tuning that was broadly tuned.

Previous studies of hippocampus activity in freely behaving pigeons did not track the head direction[43] and therefore it is not known whether HD cells can be found in other species of birds. Our study is thus unique to report HD cells in an avian species. This observation, taken together with observations of HD cells in a variety of species, ranging from insects to fish to mammals, suggests that HD cells, and not place cells, were conserved through evolution. These intriguing inter-species differences call for further comparative investigations of spatial cell types across vertebrates and linking it to the animals' behavioral repertoire and evolutionary history: a merging of neuroscience, evolution, and behavioral ecology.

STAR★METHODS

Detailed methods are provided in the online version of this paper and include the following:

- KEY RESOURCES TABLE
- RESOURCE AVAILABILITY
  - Lead contact
  - Materials availability
  - Data and code availability
- EXPERIMENTAL MODEL AND SUBJECT DETAILS
- METHOD DETAILS
  - Surgery
  - Electrophysiological recordings
  - Histology
- QUANTIFICATION AND STATISTICAL ANALYSIS
  - Data processing and spike sorting
  - Data analysis

SUPPLEMENTAL INFORMATION

Supplemental information can be found online at https://doi.org/10.1016/j.cub.2021.04.029.

ACKNOWLEDGMENTS

We thank Dr. Yael Zahar for assistance and support, and May-Britt Moser, Edvard I. Moser, and Charlotte N. Boccara for usage of rat data in Figure S3. This work was supported by research grants from the Ruth and Bruce Rappaport Institute for Biomedical Research, the Adelis Foundation, and the Israel Science Foundation. Y.G. also acknowledges the generous support of the Edward S. Mueller Eye Research Fund.

AUTHOR CONTRIBUTIONS

E.B.-Y., K.K., and S.R. conducted the experiments, wrote code, analyzed data, and produced graphs and figures. N.U., D.D., and Y.G. planned the experiments and designed the experimental setups. All authors contributed to the writing of the paper.

DECLARATION OF INTERESTS

The authors declare no competing interests.

Received: February 27, 2021
Revised: April 2, 2021
Accepted: April 12, 2021
Published: May 10, 2021

REFERENCES

1. O'Keefe, J., and Dostrovsky, J. (1971). The hippocampus as a spatial map. Preliminary evidence from unit activity in the freely-moving rat. Brain Res. *34*, 171–175.
2. O'Keefe, J., and Nadel, L. (1978). The Hippocampus as a Cognitive Map (Clarendon Press).
3. Eichenbaum, H. (2017). The role of the hippocampus in navigation is memory. J. Neurophysiol. *117*, 1785–1796.

4. Taube, J.S., Muller, R.U., and Ranck, J.B., Jr. (1990). Head-direction cells recorded from the postsubiculum in freely moving rats. I. Description and quantitative analysis. J. Neurosci. *10*, 420–435.
5. Rolls, E.T. (1999). Spatial view cells and the representation of place in the primate hippocampus. Hippocampus *9*, 467–480.
6. Hafting, T., Fyhn, M., Molden, S., Moser, M.B., and Moser, E.I. (2005). Microstructure of a spatial map in the entorhinal cortex. Nature *436*, 801–806.
7. Solstad, T., Boccara, C.N., Kropff, E., Moser, M.B., and Moser, E.I. (2008). Representation of geometric borders in the entorhinal cortex. Science *322*, 1865–1868.
8. Lever, C., Burton, S., Jeewajee, A., O'Keefe, J., and Burgess, N. (2009). Boundary vector cells in the subiculum of the hippocampal formation. J. Neurosci. *29*, 9771–9777.
9. Kropff, E., Carmichael, J.E., Moser, M.B., and Moser, E.I. (2015). Speed cells in the medial entorhinal cortex. Nature *523*, 419–424.
10. Sarel, A., Finkelstein, A., Las, L., and Ulanovsky, N. (2017). Vectorial representation of spatial goals in the hippocampus of bats. Science *355*, 176–180.
11. McHugh, T.J., Blum, K.I., Tsien, J.Z., Tonegawa, S., and Wilson, M.A. (1996). Impaired hippocampal representation of space in CA1-specific NMDAR1 knockout mice. Cell *87*, 1339–1349.
12. Ulanovsky, N., and Moss, C.F. (2007). Hippocampal cellular and network activity in freely moving echolocating bats. Nat. Neurosci. *10*, 224–233.
13. Yartsev, M.M., Witter, M.P., and Ulanovsky, N. (2011). Grid cells without theta oscillations in the entorhinal cortex of bats. Nature *479*, 103–107.
14. Killian, N.J., Jutras, M.J., and Buffalo, E.A. (2012). A map of visual space in the primate entorhinal cortex. Nature *491*, 761–764.
15. Ono, T., Nakamura, K., Nishijo, H., and Eifuku, S. (1993). Monkey hippocampal neurons related to spatial and nonspatial functions. J. Neurophysiol. *70*, 1516–1529.
16. Ekstrom, A.D., Kahana, M.J., Caplan, J.B., Fields, T.A., Isham, E.A., Newman, E.L., and Fried, I. (2003). Cellular networks underlying human spatial navigation. Nature *425*, 184–188.
17. Derdikman, D., and Knierim, J.J. (2014). Space, Time and Memory in the Hippocampal Formation (Springer).
18. Anderson, M.I., Killing, S., Morris, C., O'Donoghue, A., Onyiagha, D., Stevenson, R., Verriotis, M., and Jeffery, K.J. (2006). Behavioral correlates of the distributed coding of spatial context. Hippocampus *16*, 730–742.
19. Geva-Sagiv, M., Las, L., Yovel, Y., and Ulanovsky, N. (2015). Spatial cognition in bats and rats: from sensory acquisition to multiscale maps and navigation. Nat. Rev. Neurosci. *16*, 94–108.
20. Wiltschko, W., and Wiltschko, R. (2012). Global navigation in migratory birds: tracks, strategies, and interactions between mechanisms. Curr. Opin. Neurobiol. *22*, 328–335.
21. Mouritsen, H., Heyers, D., and Güntürkün, O. (2016). The neural basis of long-distance navigation in birds. Annu. Rev. Physiol. *78*, 133–154.
22. Thorup, K., Bisson, I.-A., Bowlin, M.S., Holland, R.A., Wingfield, J.C., Ramenofsky, M., and Wikelski, M. (2007). Evidence for a navigational map stretching across the continental U.S. in a migratory songbird. Proc. Natl. Acad. Sci. USA *104*, 18115–18119.
23. Wallraff, H.G. (2005). Avian Navigation: Pigeon Homing as a Paradigm (Springer Science & Business Media).
24. Bingman, V.P., Hough, G.E., II, Kahn, M.C., and Siegel, J.J. (2003). The homing pigeon hippocampus and space: in search of adaptive specialization. Brain Behav. Evol. *62*, 117–127.
25. Grodzinski, U., and Clayton, N.S. (2010). Problems faced by food-caching corvids and the evolution of cognitive solutions. Philos. Trans. R. Soc. Lond. B Biol. Sci. *365*, 977–987.
26. Healy, S.D., and Hurly, T.A. (2004). Spatial learning and memory in birds. Brain Behav. Evol. *63*, 211–220.
27. Healy, S.D., de Kort, S.R., and Clayton, N.S. (2005). The hippocampus, spatial memory and food hoarding: a puzzle revisited. Trends Ecol. Evol. *20*, 17–22.
28. Rinnert, P., Kirschhock, M.E., and Nieder, A. (2019). Neuronal correlates of spatial working memory in the endbrain of crows. Curr. Biol. *29*, 2616–2624.e4.
29. Herold, C., Coppola, V.J., and Bingman, V.P. (2015). The maturation of research into the avian hippocampal formation: recent discoveries from one of the nature's foremost navigators. Hippocampus *25*, 1193–1211.
30. Karten, H.J. (1969). The organization of the avian telencephalon and some speculations on the phylogeny of the amniote telencephalon. Ann. N. Y. Acad. Sci. *167*, 164–179.
31. Atoji, Y., and Wild, J.M. (2006). Anatomy of the avian hippocampal formation. Rev. Neurosci. *17*, 3–15.
32. Chen, C.C., Winkler, C.M., Pfenning, A.R., and Jarvis, E.D. (2013). Molecular profiling of the developing avian telencephalon: regional timing and brain subdivision continuities. J. Comp. Neurol. *521*, 3666–3701.
33. Colombo, M., and Broadbent, N. (2000). Is the avian hippocampus a functional homologue of the mammalian hippocampus? Neurosci. Biobehav. Rev. *24*, 465–484.
34. Rattenborg, N.C., and Martinez-Gonzalez, D. (2011). A bird-brain view of episodic memory. Behav. Brain Res. *222*, 236–245.
35. Rattenborg, N.C., Martinez-Gonzalez, D., Roth, T.C., II, and Pravosudov, V.V. (2011). Hippocampal memory consolidation during sleep: a comparison of mammals and birds. Biol. Rev. Camb. Philos. Soc. *86*, 658–691.
36. Siegel, J.J., Nitz, D., and Bingman, V.P. (2000). Hippocampal theta rhythm in awake, freely moving homing pigeons. Hippocampus *10*, 627–631.
37. Gagliardo, A., Ioalé, P., and Bingman, V.P. (1999). Homing in pigeons: the role of the hippocampal formation in the representation of landmarks used for navigation. J. Neurosci. *19*, 311–315.
38. Watanabe, S., and Bischof, H.J. (2004). Effects of hippocampal lesions on acquisition and retention of spatial learning in zebra finches. Behav. Brain Res. *155*, 147–152.
39. Smulders, T.V., and DeVoogd, T.J. (2000). Expression of immediate early genes in the hippocampal formation of the black-capped chickadee (*Poecile atricapillus*) during a food-hoarding task. Behav. Brain Res. *114*, 39–49.
40. Mayer, U., and Bischof, H.J. (2012). Brain activation pattern depends on the strategy chosen by zebra finches to solve an orientation task. J. Exp. Biol. *215*, 426–434.
41. Pravosudov, V.V., and Smulders, T.V. (2010). Integrating ecology, psychology and neurobiology within a food-hoarding paradigm. Philos. Trans. R. Soc. Lond. B Biol. Sci. *365*, 859–867.
42. Hough, G.E., and Bingman, V.P. (2004). Spatial response properties of homing pigeon hippocampal neurons: correlations with goal locations, movement between goals, and environmental context in a radial-arm arena. J. Comp. Physiol. A Neuroethol. Sens. Neural Behav. Physiol. *190*, 1047–1062.
43. Kahn, M.C., Siegel, J.J., Jechura, T.J., and Bingman, V.P. (2008). Response properties of avian hippocampal formation cells in an environment with unstable goal locations. Behav. Brain Res. *191*, 153–163.
44. Siegel, J.J., Nitz, D., and Bingman, V.P. (2006). Lateralized functional components of spatial cognition in the avian hippocampal formation: evidence from single-unit recordings in freely moving homing pigeons. Hippocampus *16*, 125–140.
45. Baylé, J.D., Ramade, F., and Oliver, J. (1974). Stereotaxic topography of the brain of the quail (*Coturnix coturnix japonica*). J. Physiol. (Paris) *68*, 219–241.
46. Poynter, G., Huss, D., and Lansford, R. (2009). Japanese quail: an efficient animal model for the production of transgenic avians. Cold Spring Harb. Protoc. *2009*, pdb.emo112.
47. Schmid, I., and Wechsler, B. (1997). Behaviour of Japanese quail (*Coturnix japonica*) kept in semi-natural aviaries. Appl. Anim. Behav. Sci. *55*, 103–112.

48. Kahn, M.C., and Bingman, V.P. (2004). Lateralization of spatial learning in the avian hippocampal formation. Behav. Neurosci. *118*, 333–344.

49. Gofman, X., Tocker, G., Weiss, S., Boccara, C.N., Lu, L., Moser, M.B., Moser, E.I., Morris, G., and Derdikman, D. (2019). Dissociation between postrhinal cortex and downstream parahippocampal regions in the representation of egocentric boundaries. Curr. Biol. *29*, 2751–2757.e4.

50. Boccara, C.N., Sargolini, F., Thoresen, V.H., Solstad, T., Witter, M.P., Moser, E.I., and Moser, M.-B. (2010). Grid cells in pre- and parasubiculum. Nat. Neurosci. *13*, 987–994.

51. Dudchenko, P.A., Goodridge, J.P., and Taube, J.S. (1997). The effects of disorientation on visual landmark control of head direction cell orientation. Exp. Brain Res. *115*, 375–380.

52. Finkelstein, A., Derdikman, D., Rubin, A., Foerster, J.N., Las, L., and Ulanovsky, N. (2015). Three-dimensional head-direction coding in the bat brain. Nature *517*, 159–164.

53. Taube, J.S., and Muller, R.U. (1998). Comparisons of head direction cell activity in the postsubiculum and anterior thalamus of freely moving rats. Hippocampus *8*, 87–108.

54. Robertson, R.G., Rolls, E.T., Georges-François, P., and Panzeri, S. (1999). Head direction cells in the primate pre-subiculum. Hippocampus *9*, 206–219.

55. Vinepinsky, E., Cohen, L., Perchik, S., Ben-Shahar, O., Donchin, O., and Segev, R. (2020). Representation of edges, head direction, and swimming kinematics in the brain of freely-navigating fish. Sci. Rep. *10*, 14762.

56. Seelig, J.D., and Jayaraman, V. (2015). Neural dynamics for landmark orientation and angular path integration. Nature *521*, 186–191.

57. Turner-Evans, D.B., and Jayaraman, V. (2016). The insect central complex. Curr. Biol. *26*, R453–R457.

58. Munn, R.G., and Giocomo, L.M. (2020). Multiple head direction signals within entorhinal cortex: origin and function. Curr. Opin. Neurobiol. *64*, 32–40.

59. Cullen, K.E., and Taube, J.S. (2017). Our sense of direction: progress, controversies and challenges. Nat. Neurosci. *20*, 1465–1473.

60. Chen, L.L., Lin, L.H., Barnes, C.A., and McNaughton, B.L. (1994). Head-direction cells in the rat posterior cortex. II. Contributions of visual and ideothetic information to the directional firing. Exp. Brain Res. *101*, 24–34.

61. Goodridge, J.P., Dudchenko, P.A., Worboys, K.A., Golob, E.J., and Taube, J.S. (1998). Cue control and head direction cells. Behav. Neurosci. *112*, 749–761.

62. Hulse, B.K., and Jayaraman, V. (2020). Mechanisms underlying the neural computation of head direction. Annu. Rev. Neurosci. *43*, 31–54.

63. Yoder, R.M., Clark, B.J., and Taube, J.S. (2011). Origins of landmark encoding in the brain. Trends Neurosci. *34*, 561–571.

64. Clark, B.J., and Taube, J.S. (2012). Vestibular and attractor network basis of the head direction cell signal in subcortical circuits. Front. Neural Circuits *6*, 7.

65. Taube, J.S. (2007). The head direction signal: origins and sensory-motor integration. Annu. Rev. Neurosci. *30*, 181–207.

66. Winter, S.S., Clark, B.J., and Taube, J.S. (2015). Spatial navigation. Disruption of the head direction cell network impairs the parahippocampal grid cell signal. Science *347*, 870–874.

67. Jacob, P.Y., Casali, G., Spieser, L., Page, H., Overington, D., and Jeffery, K. (2017). An independent, landmark-dominated head-direction signal in dysgranular retrosplenial cortex. Nat. Neurosci. *20*, 173–175.

68. Kornienko, O., Latuske, P., Bassler, M., Kohler, L., and Allen, K. (2018). Non-rhythmic head-direction cells in the parahippocampal region are not constrained by attractor network dynamics. eLife *7*, e35949.

69. Atoji, Y., and Wild, J.M. (2004). Fiber connections of the hippocampal formation and septum and subdivisions of the hippocampal formation in the pigeon as revealed by tract tracing and kainic acid lesions. J. Comp. Neurol. *475*, 426–461.

70. Krebs, J.R., Erichsen, J.T., and Bingman, V.P. (1991). The distribution of neurotransmitters and neurotransmitter-related enzymes in the dorsomedial telencephalon of the pigeon (*Columba livia*). J. Comp. Neurol. *314*, 467–477.

71. Kempermann, G. (2012). New neurons for 'survival of the fittest.'. Nat. Rev. Neurosci. *13*, 727–736.

72. Striedter, G.F. (2016). Evolution of the hippocampus in reptiles and birds. J. Comp. Neurol. *524*, 496–517.

73. Herold, C., Bingman, V.P., Ströckens, F., Letzner, S., Sauvage, M., Palomero-Gallagher, N., Zilles, K., and Güntürkün, O. (2014). Distribution of neurotransmitter receptors and zinc in the pigeon (*Columba livia*) hippocampal formation: a basis for further comparison with the mammalian hippocampus. J. Comp. Neurol. *522*, 2553–2575.

74. Atoji, Y., Sarkar, S., and Wild, J.M. (2016). Proposed homology of the dorsomedial subdivision and V-shaped layer of the avian hippocampus to Ammon's horn and dentate gyrus, respectively. Hippocampus *26*, 1608–1617.

75. Székely, A.D. (1999). The avian hippocampal formation: subdivisions and connectivity. Behav. Brain Res. *98*, 219–225.

76. Siegel, J.J., Nitz, D., and Bingman, V.P. (2002). Electrophysiological profile of avian hippocampal unit activity: a basis for regional subdivisions. J. Comp. Neurol. *445*, 256–268.

77. Shanahan, M., Bingman, V.P., Shimizu, T., Wild, M., and Güntürkün, O. (2013). Large-scale network organization in the avian forebrain: a connectivity matrix and theoretical analysis. Front. Comput. Neurosci. *7*, 89.

78. Trottier, C., Repérant, J., and Miceli, D. (1995). Anatomical evidence of a retino-thalamo-hippocampal pathway in the pigeon (*Columba livia*). J. Hirnforsch. *36*, 489–500.

79. Simonnet, J., and Fricker, D. (2018). Cellular components and circuitry of the presubiculum and its functional role in the head direction system. Cell Tissue Res. *373*, 541–556.

80. Sargolini, F., Fyhn, M., Hafting, T., McNaughton, B.L., Witter, M.P., Moser, M.-B., and Moser, E.I. (2006). Conjunctive representation of position, direction, and velocity in entorhinal cortex. Science *312*, 758–762.

81. Giocomo, L.M., Stensola, T., Bonnevie, T., Van Cauter, T., Moser, M.B., and Moser, E.I. (2014). Topography of head direction cells in medial entorhinal cortex. Curr. Biol. *24*, 252–262.

82. Güntürkün, O. (1997). Avian visual lateralization: a review. Neuroreport *8*, iii–xi.

83. Payne, H.L., Lynch, G.F., and Aronov, D. (2020). Precise spatial representations in the hippocampus of a food-caching bird. bioRxiv. https://doi.org/10.1101/2020.11.27.399444.

84. Ruploh, T., Kazek, A., and Bischof, H.J. (2011). Spatial orientation in Japanese quails (*Coturnix coturnix japonica*). PLoS One *6*, e28202.

85. Cheng, K., Spetch, M.L., Kelly, D.M., and Bingman, V.P. (2006). Small-scale spatial cognition in pigeons. Behav. Processes *72*, 115–127.

86. Mayer, U., Watanabe, S., and Bischof, H.J. (2013). Spatial memory and the avian hippocampus: research in zebra finches. J. Physiol. Paris *107*, 2–12.

87. Moser, M.B., Rowland, D.C., and Moser, E.I. (2015). Place cells, grid cells, and memory. Cold Spring Harb. Perspect. Biol. *7*, a021808.

88. Catania, K.C., and Henry, E.C. (2006). Touching on somatosensory specializations in mammals. Curr. Opin. Neurobiol. *16*, 467–473.

89. Slotnick, B. (2001). Animal cognition and the rat olfactory system. Trends Cogn. Sci. *5*, 216–222.

90. Shimizu, T., Patton, T.B., and Husband, S.A. (2010). Avian visual behavior and the organization of the telencephalon. Brain Behav. Evol. *75*, 204–217.

91. Geva-Sagiv, M., Romani, S., Las, L., and Ulanovsky, N. (2016). Hippocampal global remapping for different sensory modalities in flying bats. Nat. Neurosci. *19*, 952–958.

92. Lormant, F., Cornilleau, F., Constantin, P., Meurisse, M., Lansade, L., Leterrier, C., Lévy, F., and Calandreau, L. (2020). Research note: role of the hippocampus in spatial memory in Japanese quail. Poult. Sci. *99*, 61–66.

93. Bingman, V.P., and Yates, G. (1992). Hippocampal lesions impair navigational learning in experienced homing pigeons. Behav. Neurosci. *106*, 229–232.

94. Mayer, U., Watanabe, S., and Bischof, H.J. (2010). Hippocampal activation of immediate early genes Zenk and c-Fos in zebra finches (*Taeniopygia guttata*) during learning and recall of a spatial memory task. Neurobiol. Learn. Mem. *93*, 322–329.

95. Sherry, D.F., Grella, S.L., Guigueno, M.F., White, D.J., and Marrone, D.F. (2017). Are there place cells in the avian hippocampus? Brain Behav. Evol. *90*, 73–80.

96. Karten, H.J., and Hodos, W. (1967). A Stereotaxic Atlas of the Brain of the Pigeon (*Columba livia*) (The Johns Hopkins Press).

97. Weiss, S., Talhami, G., Gofman-Regev, X., Rapoport, S., Eilam, D., and Derdikman, D. (2017). Consistency of spatial representations in rat entorhinal cortex predicts performance in a reorientation task. Curr. Biol. *27*, 3658–3665.e4.

98. Schmitzer-Torbert, N., Jackson, J., Henze, D., Harris, K., and Redish, A.D. (2005). Quantitative measures of cluster quality for use in extracellular recordings. Neuroscience *131*, 1–11.

99. Skaggs, W.E., McNaughton, B.L., Wilson, M.A., and Barnes, C.A. (1996). Theta phase precession in hippocampal neuronal populations and the compression of temporal sequences. Hippocampus *6*, 149–172.

Please cite this article in press as: Ben-Yishay et al., Directional tuning in the hippocampal formation of birds, Current Biology (2021), https://doi.org/10.1016/j.cub.2021.04.029

STAR★METHODS

KEY RESOURCES TABLE

REAGENT or RESOURCE	SOURCE	IDENTIFIER
Deposited data		
Spike trains of all single units and corresponding behavioral data.	This paper	Mendeley Data: https://dx.doi.org/10.17632/hs2nbsw5vy.1
Experimental models: Organisms/strains		
Japanese quails (Coturnix japonica)	Self-breeding	N/A
Software and algorithms		
Spike sorting software	Neuralynx	SpikeSort3D
MATLAB	The Mathworks	https://www.mathworks.com
Other		
Skull adhesive cement	C&B-metabond	http://www.parkell.com/c-b-metabond_3
Silicon coat to cover exposed brain surface	Kwik-Sil	https://www.wpiinc.com/kwik-sil-low-toxicity-silicone-adhesive
Light cure dental resin	Spident EsFlow	http://spidentusa.com/index.php/es-flow.html
Bone screws	FST 4 mm self-tapping screws	https://www.finescience.com/en-US/Products/Bone-Instruments/Bone-Screws/Self-Tapping-Bone-Screws
Wires for tetrodes	California Fine Wire	Model:M283720 size: 17.8 μm, Platinum 90% Iridium 10%
Custom made microdrives	Parts manufacture by Rogat Enterprises	3D designs and assembly protocols can be obtained upon request
Tethered acquisition system	Neuralynx Digital Lynx SX platform	https://neuralynx.com/
Non-tethered acquisition system (Neural logger)	Deuteron Technologies, MouseLog-16	https://deuterontech.com/

RESOURCE AVAILABILITY

Lead contact

Further information and requests for resources and reagents should be directed to and will be fulfilled by the lead contact, Yoram Gutfreund (yoramg@technion.ac.il).

Materials availability

This study did not generate new unique reagents.

Data and code availability

The dataset of the spike trains of the single units generated in this study, the behavioral data and the results of the analysis are available at Mendeley Data: https://dx.doi.org/10.17632/hs2nbsw5vy.1

This study did not generate a unique code.

EXPERIMENTAL MODEL AND SUBJECT DETAILS

Adult Japanese quails (*Coturnix japonica)* of both sexes were used in this study (females and males; weight: 150 – 250 g, age: 4 – 12 months). The quails were hatched and raised in our in-house breeding colony, housed in 1x1 m cages and maintained on

Please cite this article in press as: Ben-Yishay et al., Directional tuning in the hippocampal formation of birds, Current Biology (2021), https://doi.org/10.1016/j.cub.2021.04.029

a 12/12hr light/dark cycle. Food and water were provided *ad libitum*. All procedures were in accordance with the ethical guidelines and were approved by the Technion Institutional Animal Care and Use Committee. During recording sessions, no painful procedures were carried out.

METHOD DETAILS

Surgery

Quails were prepared for repeated electrophysiological recordings with a single surgical procedure: the birds were anaesthetized with 3% isoflurane in a 4:5 mixture of nitrous oxide and oxygen. Quails were then positioned in a stereotaxic frame (Kopf, small animals instrument Model 963) using Kopf rat ear bars. Head angle was controlled with a biting bar that was positioned 45° below the inter-aural axes (resembling the standard position in the pigeon and the quail atlases.[45,96] At this head position, in our stereotaxic setup, the cerebellum rostral tip was found at coordinate 0 (inter-aural line) ± 0.5 mm rostro-caudal. During surgery, animal temperature was maintained using a closed-circuit heating pad. Lidocaine (Lidocaine HCl 2% and Epinephrine) was injected locally at the incision site. The skull was exposed and cleaned. Two to four skull screws were inserted at the caudal part of the skull and one ground screw was inserted at the right frontal part of the skull. A 2 mm craniotomy was performed, in various positions ranging up to 4 mm rostral from the inter-aural line, and a small nick in the dura was made at the center of the craniotomy with a surgical needle. A custom-made microdrive (as described in Weiss et al.[97]) containing four tetrodes (made of 17.8-μm platinum-iridium wire, California Fine Wire) was carefully lowered until the tetrodes smoothly entered the brain tissue. Antibiotic ointment (Chloramfenicol 5%) was applied to the brain surface, followed by a thin silicon coat (Kwik-Sil). The drive was then connected to the ground screw with a silver-wire and attached to the skull with adhesive cement (C&B-metabond) and light cured dental resin (Spident EsFlow). Loxicom (5mg/ml) was injected intramuscularly and the quails were positioned in a heated chamber to recover overnight.

Electrophysiological recordings

Electrophysiological recordings were conducted in a 1 × 1 m open-field wooden arena with black walls and floor (wall height 0.7 m). The arena was positioned in a small windowless room, and was typically illuminated from above, or in some experiments from a light source positioned in one of two corners of the arena, 90 cm above the ground. A black curtain separated the arena on one side from the experimental rig and the experimenter; the other three sides were open to the room interior, which included many landmarks in multiple directions, such as electrical outlets, shelves, a door etc. The birds were released to roam spontaneously in the arena. Occasionally, food items were scattered in the arena to encourage movement. A tethered 16-channel head-stage (Intan RHD2132) was attached to the drive and connected through a commutator (Saturn) to a data acquisition system (Neuralynx Digital SX). In some of the experiments the quails were untethered, in which case a 16-channel neural-logger (Deuteron Technologies, MouseLog-16) was used for on-board acquisition and data storing. In both cases, animals were filmed with a CCTV camera with a frame-rate of 25Hz, and their position and head orientation was tracked by video-tracking two LEDs (green and red) mounted on both sides of the head-stage or the neural-logger. Recording sessions were performed daily and lasted 10–45 minutes. Tetrodes were advanced by 50 μm per day. If no spikes were detected, electrodes were continuously lowered until spikes were observed. After reaching a depth of near 1000 μm, in some of the experiments, electrodes were retracted to regions of previously observed spiking activity and additional experiments were conducted. The thickness of the quail HPF layer varies from ~800 μm on the lateral side to ~2000 μm on the medial side.[45] Therefore recording depth was restricted to within 1200 μm below the brain surface, with more than 80% of the neurons collected in depths between 200 to 800 μm (Figure 5B). Thus, the bulk of the recorded population of neurons was collected within the HPF. Yet, we cannot rule out the possibility that a small subset of the neurons from deep sites were recorded below the lateral ventricle, or that neurons in the most lateral penetrations were from bordering areas adjacent to the HPF.

Electrical recording was sampled at 30 kHz using the Cheetah 6.0 software (Neuralynx), which records both 16-channel continuous raw data and spike waveforms. Raw signals were pre-amplified, bandpass filtered to 300 – 3000 Hz and thresholded (30 – 60μV) to obtain on-line spiking activity (see Figure S5 for examples of filtered traces). In untethered recordings, signals from the 16 channels of the neural-logger were amplified (×200), filtered (300 – 7000 Hz) and sampled continuously at 29.3 kHz or 31.25 kHz per channel, and stored on-board. For synchronization between the neural-logger data recording and the Neuralynx video recording, a neural-logger control box sent TTL pulses to both the neural-logger and Neuralynx system at random intervals (10 ± 5 s). The timestamps were synchronized by utilizing polynomial curve fitting between the pulses recorded on both systems.

Histology

In a few of the quails, an electrical lesion was performed by injecting a positive current through one of the tetrodes (+5 μA for 20 s). A week later, the quail was deeply anesthetized and perfused with phosphate buffer solution (PBS) followed by 4% paraformaldehyde. The brain was removed and stored in 4% paraformaldehyde for 2–3 days at 4°C, then transferred to PBS. Following fixation, the quail brains were dehydrated in 70%, 80%, 95% and 100% ethanol, cleared in Xylene and embedded in paraffin wax. The paraffin-embedded brains were coronal sectioned at 5 μm using a microtome (RM 2265 Leica). Sections collected at 40 μm intervals were mounted on superfrost glass slides and dried in an oven at 37°C for 24 hours. After drying the sections, they were deparaffinized in xylene, rehydrated in a diluted ethanol series, and stained with 0.1% Cresyl violet solution (Nissl stain). The sections were then dehydrated, cleared and coverslipped with DPX mounting medium (Merck).

Please cite this article in press as: Ben-Yishay et al., Directional tuning in the hippocampal formation of birds, Current Biology (2021), https://doi.org/10.1016/j.cub.2021.04.029

QUANTIFICATION AND STATISTICAL ANALYSIS

Data processing and spike sorting

During subsequent processing (offline), the electrical recordings were filtered between 600 – 6,000 Hz, and an adaptive voltage threshold (Thr) was used for spike detection:

$$\mathrm{Thr} = 4^{*}\mathrm{median}\left\{\frac{|x|}{0.6745}\right\}$$

Where *x* is the filtered recorded signal. The division by 0.6745 accounts for the relationship between the median of the noise and the standard deviation of a normal distribution. Voltage threshold was calculated over 1 minute recording windows. Electrical artifacts were detected and removed from all channels based on absolute voltage. Following artifact removal, a spike detection algorithm was used for each tetrode: whenever one channel crossed the threshold value, a 1-ms wide segment was saved from all channels on the tetrode, where the peak was centered over the 8th sample (for a total of 32 samples). Coincidence detection algorithm was used to further identify and remove movement artifacts; large-amplitude events occurred within all channels in each tetrode or between tetrodes were removed from analysis (Figure S5B). Additionally, all detected spikes were compared to a pre-existing spike-shape database (*template matching*) by correlating different segments of the spike shape to each template from the database. A spike was included for further analysis if its Pearson-correlation coefficient with any of the spike templates was larger than 0.8.

Manual spike sorting was performed offline using SpikeSort3D software (Neuralynx) and consisted of plotting the spikes in 3D parameter space, finding the features which give the best cluster separation and performing manual cluster cutting. Clustering quality was assessed based on two measures: isolation distance and L_{ratio}.[98] These parameters estimate how well-separated is the cluster of spikes from the other spikes and noise recorded on the same tetrode. A well-separated cluster has a large isolation distance and a small L_{ratio}. A cluster was considered a single unit if it had an L_{ratio} smaller than 0.2 and an isolation distance larger than 15. When the number of points outside the isolated cluster is smaller than half of the total points in the tetrode it is not possible to obtain the isolation distance value (NaN isolation distance). Clusters with NaN isolation distance were included in the analysis (Table S2). Additionally, clusters were categorized as multi- or single-units based on their inter-spike interval histogram: a cluster was categorized as single-unit if less than 5% of its spikes occurred less than 2 ms after the previous spike.

Data analysis

Single units were included for further analysis only if at least 300 spikes occurred during the session, and the recording session lasted more than 10 minutes.

Spatial firing-rate maps were computed by partitioning the arena into 3x3 cm bins. The number of spikes in each bin was divided by the time the bird spent in that bin. Bins which the quail visited for less than 200 ms were discarded and were colored white in the firing-rate map. Experiments in which the quail visited less than 50% of the arena were discarded from the spatial rate-map analysis. Spatial modulation was assessed based on two common measures: spatial information and spatial correlation.[99] Spatial information index was calculated as:

$$I = \sum_{x} \frac{p_x \lambda_x \log_2\left(\frac{\lambda_x}{\lambda}\right)}{\lambda}$$

Where λ is the mean firing rate of the cell, λ_x is the mean firing rate in bin *x* (x includes only bins that the quail visited), p_x is the probability of occupying bin *x*. Spatial correlation was the 2-dimensional correlation coefficient between the rate map of the first and second halves of the session – an index of stability. For statistical evaluation of the spatial modulation, a randomization procedure was applied. The entire spike train was rigidly and circularly shifted by a random interval (intervals smaller than ± 20 s were not used). This was repeated 1000 times for each neuron, and for each of the shifts the spatial information index was calculated. The experimentally observed index for the actual neuron was considered statistically significant with a p value smaller than 0.01 if it surpassed 99% of the shuffle indices. For display purposes, the rate maps were smoothed using a 2D Gaussian kernel (σ = 1 bins), but all the computations and indexes were calculated without smoothing.

Head-direction was computed as the perpendicular orientation from the line connecting the positions of the two LEDs (we used the red and green colors of the LEDs to unambiguously determine the correct direction). Head direction data were binned at 6° bins. The number of spikes in each bin was divided by the time the animal spent at that direction. The histogram was smoothed using a hamming window (n = 10 points) and displayed in polar plot view.

To assess the directionality of the tuning curve, the mean vector length of the circular distribution (Rayleigh vector) was calculated:

$$R = \frac{\left|\sum w \times e^{i\alpha}\right|}{\sum w}$$

Where *w* is the firing-rate per bin and α is the bin direction. The preferred (mean) direction of the tuning curve was estimated by the direction of the Rayleigh vector:

$$\text{preferred direction} = \mathrm{Arg}\left(\sum w \times e^{i\alpha}\right)$$

Please cite this article in press as: Ben-Yishay et al., Directional tuning in the hippocampal formation of birds, Current Biology (2021), https://doi.org/10.1016/j.cub.2021.04.029

The statistical significance of the directionality was assessed by applying a spike-shuffling procedure as described above. Shuffling was repeated 1000 times, and for each shuffle the Rayleigh vector (RV) length was calculated. A neuron was considered head-direction modulated if the RV score was larger than 99% of the shuffled scores. A shuffling procedure was used only for tuning curves with a RV score higher than 0.10.

The stability of the HD preferred direction was assessed by dividing the time of the experiment into two halves (Figure 3D); by dividing the arena into two regions: south half versus north half, east half versus west half, and center region versus border region (Figures 3E–3G); and by dividing the quail's speed to two speeds: below 5 cm/sec and above 5 cm/sec (Figure 3H). Preferred HD was calculated separately for each part. This analysis was performed only for the sessions where the head direction coverage was larger than 50% in both regions. Head direction coverage was calculated by dividing the time spent at each region by 60 (the number of 6° HD bins) and thus obtaining the expected time at each direction-bin if the behavioral head directions were uniformly distributed. The percent coverage was then defined as the percentage of directional bins in which the quail spent more than 75% of the expected uniform time (see Figure S1 for examples).